Vol 14 No 3, March 2005
1009-1963/2005/14(03)/0604-06

Chinese Physics

© 2005 Chin. Phys. Soc.
and IOP Publishing Ltd

Dependence of the coercivity of $La_{0.67}Ca_{0.33}MnO_3$ films on substrate and thickness*

Xiong Chang-Min(熊昌民)†, Sun Ji-Rong(孙继荣), Wang Deng-Jing(王登京), Liu Guan-Juan(刘光娟), Zhang Hong-Wei(张宏伟), and Shen Bao-Gen(沈保根)

Beijing National Laboratory for Condensed Matter Physics, Institute of Physics, Chinese Academy of Sciences, Beijing 100080, *China*

(Received 31 August 2004; revised manuscript received 16 November 2004)

We investigate the effects of strain and film thickness on the coercivity of $La_{0.67}Ca_{0.33}MnO_3$ films grown on $SrTiO_3$ and $LaAlO_3$ substrates. Textured microstructure with the grain [001] pseudo-cubic axis normal to the film surface is obtained. The average grain size decreases with decreasing film thickness t. The magnetic anisotropy depends upon the substrate-induced strain. Firstly, the intrinsic coercivity ${}_iH_C$ increases as t varies from 5 nm to 10 nm, then attains a maximum at $t \sim$ 10–25nm. A further increase in t yields a gradual reduction of ${}_iH_C$. By the analysis of the dependence of ${}_iH_C$ on the measured direction of magnetic field, the coercivity mechanism is assumed to be mainly determined by the nucleation of reversed domain and the domain wall pining for $t \leq$10nm and $t \geq$25nm, respectively, which were further verified by the investigation of the initial magnetization curves for the LCMO/STO films with t=5, 10, 25 and 400nm, and the minor magnetic loops for the LCMO/LAO films with t=5 and 50nm. Moreover, the size of the inhomogeneous region in which the nucleation or pinning takes place is discussed.

Keywords: manganite film, thickness, magnetic anisotropy, coercivity
PACC: 7570, 7560, 8115, 7530V

1. Introduction

Manganite thin films have been studied intensively during the last decade since the discovery of colossal magnetoresistance (CMR). Both the underlying physics and the practical applicability of the CMR effects are the reasons for their receiving extensive attention.[1−7] Information on the magnetization behaviour of these films, such as magnetic anisotropy and coercivity, is clearly helpful for the design and fabrication of hetero-epitaxy devices such as spin valve and tunnelling junctions, etc. With regard to anisotropy, it is well established that a compressively strained film will exhibit an out-of-plane magnetization, while a film with a tensile strain favors an in-plane spin alignment.[7−11] Coercivity, especially that of ultrathin films, is another important magnetic parameter for these applications because the magnetoresistance effect is usually related to the reversal of the magnetic moment in magnetic field. In addition to the magnetic anisotropy, strain imposed by substrate, microstructure factors such as lattice defects near interfaces, and grain sizes in the film, will all affect the coercivity of the film. Thus, the investigation of the coercivity of the manganites films is a necessary preparation for their further applications. Steren *et al*[11] investigated the in-plane coercivity of $La_{0.7}Sr_{0.3}MnO_3$ film, and suggested that the coercivity varies with film thickness t as $1/t$ when t increases from about 18nm to 500nm. By a qualitative analysis, they ascribed the coercivity mechanism to the inhomogeneous pinning of domain wall. But up to now, whether the behaviours mentioned by Steren *et al* are universal in other manganites film remains open question, especially for the ultra thin films. Thus, the coercivity of manganite films is still an interesting topic, and requiring further systematic study.

$La_{0.67}Ca_{0.33}MnO_3$ (LCMO) material is one of the best studied materials, and the properties associated with the CMR effect in this material are usually focus of those studies. However, the coercivity of LCMO,

*Project supported by the Funds of Outstanding Young Researchers from the National Science Foundation of China (Grant No 50225209) and the State Key Project from the National Natural Science Foundation of China (Grant No 19934010).
†Corresponding author. E-mail: cmxiong@g203.iphy.ac.cn

especially that of LCMO films, has received less attention before. Therefore, the LCMO film is chosen as the object in this work. The magnetic anisotropy was found to be dependent on the character of substrate and the film thickness t was adjusted from 5nm to 400nm. The coercivity of LCMO films is extensively discussed in terms of magnetic anisotropy and microstructure.

2. Experiments

The LCMO films were grown on [001] $SrTiO_3$ (LCMO/STO) and (001)$LaAlO_3$ (LCMO/LAO) substrates by pulsed laser deposition. The substrate was kept at 1073K under the O_2 partial pressure of 200Pa during deposition. The film thickness was controlled by the deposition time. After deposition, the film was cooled to room temperature in an oxygen atmosphere of 200Pa. Surface morphology of the film was studied by atomic force microscopy (AFM). The crystalline structure of the samples was characterized by x-ray diffraction using the Rigaku diffractometer with Cu Kα radiation. The magnetization measurements were performed in a commercial SQUID magnetometer at temperature of 5K, and the diamagnetic substrate effects were corrected.

3. Results and discussion

As shown by the AFM images, the average grain size d decreases with the decrease of t for both the LCMO/STO and LCMO/LAO films. As examples, AFM images of the LCMO/STO films with t=150 nm and t=10 nm are displayed in Fig.1. The values of d are about 550nm and 100nm for t=150nm and 10nm, respectively.

Analysis of the x-ray diffraction pattern shows that the grains in the film are strongly textured with the (001) pseudo-cubic axis normal to the surface of the film. Figure 2 shows the thickness dependence of the out-of-plane lattice parameter c. The value of c for the LCMO/STO film is smaller than 0.7710 nm for the bulk LCMO, which implies the existence of the tensile strain. The relaxation of the tensile strain in LCMO/STO films is revealed by the monotonic increase of c with increasing t. On the contrary, the value of c for LCMO/LAO film is larger than that for the bulk, which implies the existence of compressive strain, which is also relaxed since the value of decreases with increasing t. It is interesting that c increases almost continuously from 0.7591nm to 0.7825nm with the variation of t for the two kinds of substrates.

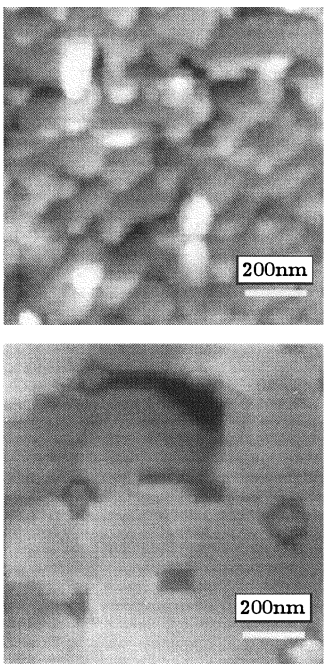


Fig.1. AFM images for the LCMO/STO films with t=10 nm (top) and 150nm (bottom).

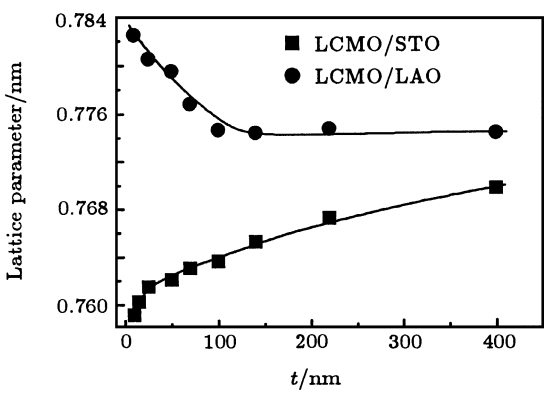


Fig.2. Out-of-plane lattice parameters of the films as functions of t.

Figure 3 shows the selected isothermal magnetization M as a function of magnetic field $H(M(H))$, measured at 5K along the [100] and [001] directions of the LCMO/STO and LCMO/LAO films with t=70nm, respectively. The out-of-plane magnetization has been corrected for the demagnetization effects. An interesting observation is the different manner for the system to approach the magnetic saturation M_S along different directions. For the LCMO/STO films, for example, M increases steeply along the [100] direction, and reaches the value of M_S rapidly. In contrast, when the field is applied along the [001] axis, M rises slowly towards the saturation state. The magnetization along the [110] has also been measured and compared with

that along [100], and no visible difference was observed. All these reveal the easy plane character of the magnetic anisotropy in the LCMO/STO films. On the contrary, the LCMO/LAO film exhibits a uniaxial anisotropy, with the easy axis directing to the film normal. This observation is consistent with the conclusion obtained by Kwon *et al*[7] that the magnetic anisotropy is related to the strain in the film. As a consequence, the magnetic anisotropy constant Ku can be calculated by $Ku = \int_{(001)} H\mathrm{d}M - \int_{(100)} H\mathrm{d}M$, with the integration performed along the $M(H)$ curves in the [100] and [001] directions, respectively. Interestingly, Ku displays a maximum at $t \sim$ 50–70nm for both the LCMO/STO and the LCMO/LAO films. The origin of the small Ku in ultra thin films is still unclear.[8–11] Further work including the study of the surface effect is required to elucidate this behaviour. For thick films, the small value of Ku can be attributed to the reduction of the strains as displayed in Fig.2.[11] Here, what we are concerned about is the variation of magnetic anisotropy field H_A, defined as H_A=2|Ku|/M_S, which is shown in Fig.4. It is obvious that the variation of H_A is mainly dominated by Ku. The maximum value of $\mu_0 H_\mathrm{A}$, occurring at t ~50–70nm, is ~0.23T for both series of films.

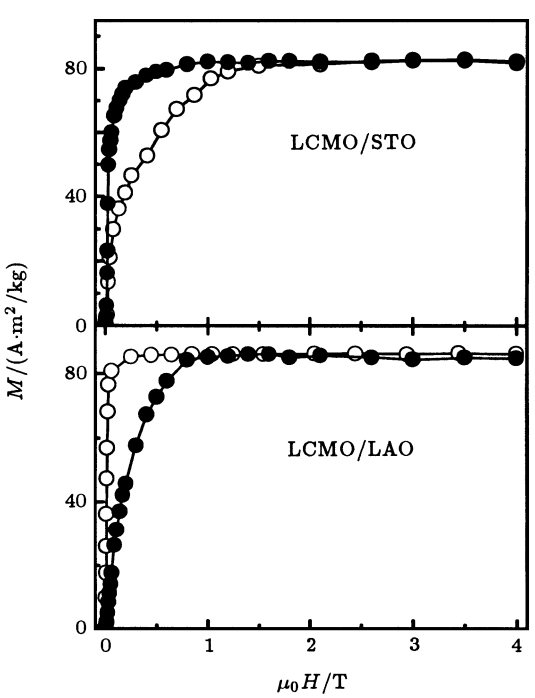


Fig.3. Selected isothermal magnetization for LCMO/STO (top) and LCMO/LAO (bottom) with t=70nm, measured at T=5K with the magnetic field parallel to (solid circles) and normal to (open circles) the film plane.

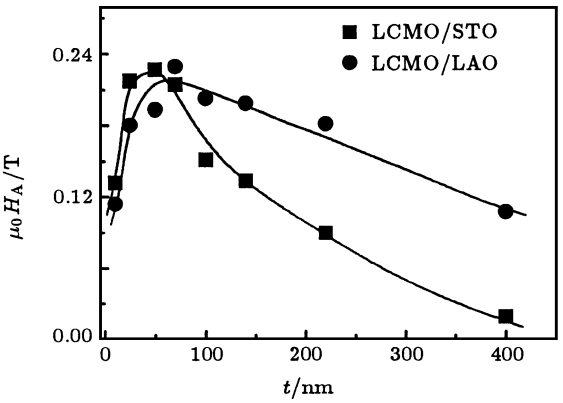


Fig.4. Magnetic anisotropy field for LCMO/STO and LCMO/LAO as functions of t.

The intrinsic coercivities ${}_{\mathrm{i}}H_{\mathrm{C}//}$ and ${}_{\mathrm{i}}H_{\mathrm{C}\perp}$ are determined from the magnetic hysteresis loops measured with the magnetic field parallel and perpendicular to the film plane, respectively. As examples, the magnetic hysteresis loops for the LCMO/STO and LCMO/LAO films with t=70nm are shown in Fig.5. The dependence of the intrinsic coercivity on t for LCMO/STO and LCMO/LAO are shown in Fig.6. The minimum value of $\mu_{0\mathrm{i}}H_\mathrm{C}$ is greater than 0.01T, while the magnitude of $\mu_{0\mathrm{i}}H_\mathrm{C}$ is usually 0.001T for bulk materials. This discrepancy is attributed to the difference in the structure features of bulk and thin films.[8–11] One observation of present study is that the coercivity increases as t varies from 5nm to 10nm. Then the coercivity gains a maximum at t ~10–25nm. A further increase in t yields a gradual reduction of coercivity for $t >$ 25nm. The relation between ${}_{\mathrm{i}}H_\mathrm{C}$ and t for thick films (inset of Fig.6) can be well described by the equation

$$ {}_{\mathrm{i}}H_\mathrm{C} = H_\mathrm{b} + \frac{P}{t^\beta}, \qquad (1) $$

where H_b is the extrapolated bulk coercivity and P a constant that depends on the film substrate and growth condition. The fitting parameter β is $\sim 1/2$. The values of $\mu_0 H_{\mathrm{b}//}$ and $\mu_0 H_{\mathrm{b}\perp}$ are 0.011T and 0.010T for the LCMO/STO films measured with the field parallel and perpendicular to the film plane, respectively. For the LCMO/LAO films, the corresponding values of $\mu_0 H_{\mathrm{b}//}$ and $\mu_0 H_{\mathrm{b}\perp}$ are 0.014T and 0.016T, respectively. As expected, there is little difference between $H_{\mathrm{b}//}$ and $H_{\mathrm{b}\perp}$. All the values of H_b are in the same order with that reported in Ref.[8]. However, β is equal to 1 according to the result in Ref.[11], suggesting that β is also dependent on the growth condition. In other words, this finding suggests that the $1/t$ dependence of coercivity is not a universal phenomenon for other manganite films. Generally, the

coercivity is affected by the factors such as the magnetic anisotropy, strain imposed by substrate, lattice defects, grain size, and surface roughness, etc. Therefore, all these factors are the possible reasons for the variation of P and β. To give a quantitative explanation for the change of P and β, further theoretical investigation is required. Giving a qualitative description and explanation of the variation of coercivity is the purpose of this study.

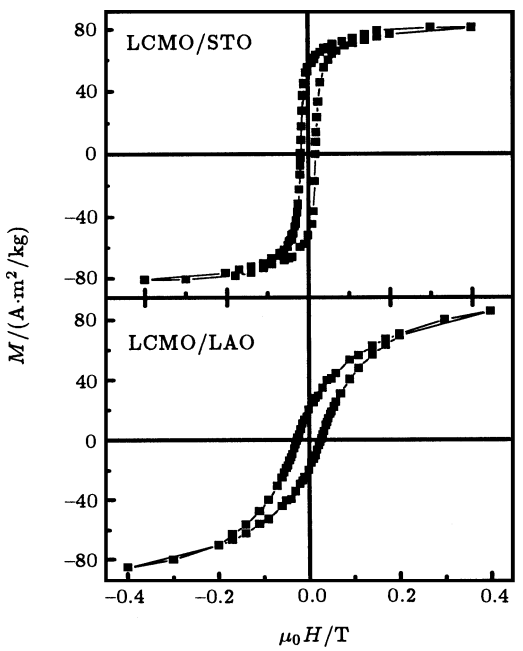


Fig.5. Magnetization hysteresis loops for LCMO/STO (top) and LCMO/LAO (bottom) with t=70nm, measured with the magnetic field parallel to the film planes.

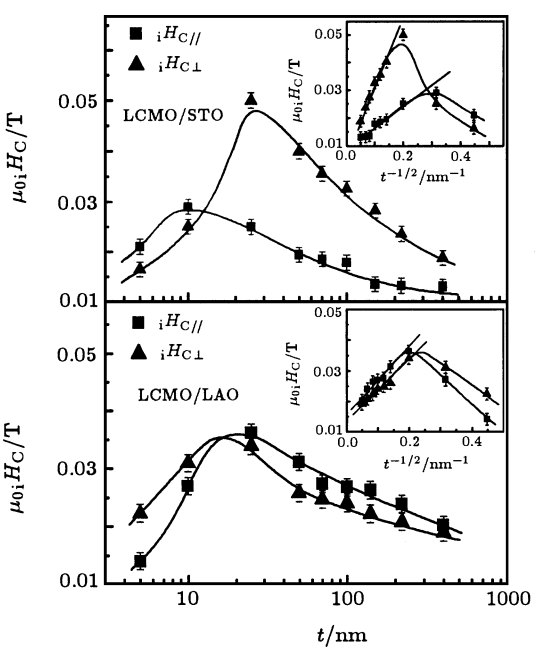


Fig.6. Intrinsic coercivity ${}_{\rm i}H_{\rm C//}$ and ${}_{\rm i}H_{\rm C\perp}$ as functions of t for LCMO/STO (top) and LCMO/LAO (bottom). Insets: intrinsic coercivity vs $1/t^{1/2}$.

Another interesting observation is that there is a difference between ${}_{\rm i}H_{\rm C//}$ and ${}_{\rm i}H_{\rm C\perp}$. For the thin LCMO/STO films with $t \leq$10nm, ${}_{\rm i}H_{\rm C//} > {\rm i}H_{\rm C\perp}$. After the coercivity goes through the maximum value at $t \sim$ 25nm, ${}_{\rm i}H_{\rm C//}$ turns out to be smaller than ${}_{\rm i}H_{\rm C\perp}$. Moreover, the difference between ${}_{\rm i}H_{\rm C//}$ and ${}_{\rm i}H_{\rm C\perp}$ can be as large as ~30% at t ~25nm. Similar case is also found for the LCMO/LAO films except that the relation between ${}_{\rm i}H_{\rm C//}$ and ${}_{\rm i}H_{\rm C\perp}$ is contrary to that for the LCMO/STO films. The intrinsic coercivity is usually analysed according to the well-known modified Brown formula[12,13]

$$ {}_{\rm i}H_{\rm C} = \alpha_{\rm k}\alpha_{\phi}\frac{2Ku}{\mu_0 M_{\rm S}} - N_{\rm eff}M_{\rm S}, \qquad (2) $$

where $\alpha_{\rm k}$ depends on the nature and size of the defect regions in which nucleation or pinning takes place, and α_{ϕ} takes account of the misalignment of the grains in the magnet, and $N_{\rm eff}$ is the averaged local effective demagnetization factor. When the angle ϕ between the applied field and easy magnetization direction increases from zero, the value of α_{ϕ} increases and decreases for the coercivity mechanism of domain wall pinning and nucleation, respectively.[12,13–16] As a result, the coercivity along the hard axis is larger(smaller) than the one along the easy axis for the coercivity mechanism of domain wall pinning (nucleation). According to the analysis of the magnetic anisotropy, ${}_{\rm i}H_{\rm C//}$ and ${}_{\rm i}H_{\rm C\perp}$ are the coercivity along the easy axis for LCMO/STO and LCMO/LAO films, respectively. Considering the relation between ${}_{\rm i}H_{\rm C//}$ and ${}_{\rm i}H_{\rm C\perp}$, it follows that the magnetization reversal is mainly controlled by nucleation of magnetic reversed domain for $t \leq$10 nm for both of the films, while the coercivity is determined by the mechanism of domain wall pinning for $t \geq$ 25nm. Similarly, Callegaro and Puppin[17] have proposed different micro–magnetic reversal process in Ni films: magnetic moment rotation for thin film and domain wall movement for thick films. Only domain wall pinning is found in the $La_{0.7}Sr_{0.3}MnO_3$ film,[10,11] which may be due to the large value of t in Ref.[11].

To gain a further insight into the magnetic reversal progress, the initial magnetization curves for the LCMO/STO films with selected t=5, 10, 25 and 100nm were investigated. As depicted in Fig.7, it is obvious that the magnetization for the three films with $t \geq$10nm shows a rapid increase at the field around the value of intrinsic coercivity, which suggests the

occurrence of the domain wall pinning in the magnetic reverse process. Notably, as t decreases from 100nm to 10nm, the magnetization tends to rise more slowly. Transmission electron microscopy has proved that, due to the lattice mismatch between the substrate and film, more defects are found in the thinner films. These defects generally act as the pining centers. Therefore, the slow increase in the magnetization for thin films can be qualitatively understood in terms of the dominating mechanism of the domain wall pining. However, compared with the 10nm film, the magnetization for LCMO with t=5nm shows a rapid increase in the magnetization (though more defects are expected in the ultra thin film), which implies that factors other than the pining mechanism are in play in the variation of the initial magnetization. In fact, the nucleation of magnetic reversed domain is another important factor affecting the magnetic reversal process, which usually leads to a fast rise of the magnetization against the magnetic field. Thus, the presence of nucleation mechanism could be the reason for the abnormal rapid increase in the magnetization for the film with t=5nm. Actually, it is highly likely that the nucleation mechanism is the dominating factor affecting the magnetic reversal progress in the ultra thin films, which is consistent with the analysis of the relation between ${}_{\rm i}H_{\rm C//}$ and ${}_{\rm i}H_{\rm C\perp}$

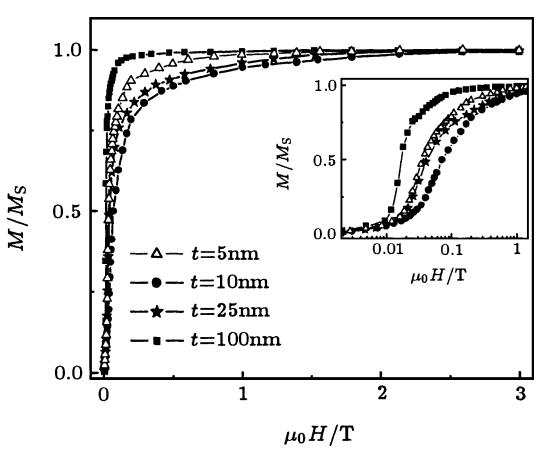


Fig.7. Initial magnetization curves for the LCMO/STO films with t= 5, 10, 25 and 100nm. Inset: a close view of the initial magnetization curves in the low magnetic field region.

The minor magnetic loops for the LCMO/LAO films with t=5 and 50nm were measured through one cycle between a maximum field $H_{\rm max}$ and $-H_{\rm max}$. Then, the dependence of remanence $M_{\rm r}(H_{\rm max})$ and coercivity $H_{\rm C}(H_{\rm max})$ are obtained, as shown in Fig.8. For the LCMO/LAO film with t=5nm, as $H_{\rm max}$ increases, $M_{\rm r}(H_{\rm max})$ approaches the saturation state more rapidly than $H_{\rm C}(H_{\rm max})$, which is a key feature of the coercivity mechanism determined by the nucleation. On the contrary, for the LCMO/LAO film with t=50nm, $H_{\rm C}(H_{\rm max})$ shows a more rapid increase towards the saturation state than $M_{\rm r}(H_{\rm max})$, confirming the domain-wall-pinning-controlled coercivity in the film.[18]

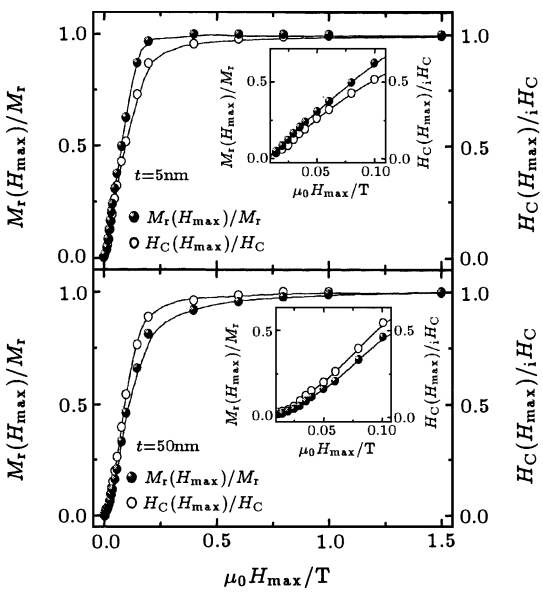


Fig.8. Comparison of the $H_{\rm max}$ dependence of $M_{\rm r}(H_{\rm max})$ and $H_{\rm C}$(H$_{\rm max}$) for the LCMO/LAO film with t=5 and t=50nm. Inset: a close view of the comparison in the low magnetic field region.

Based on the analysis of $H_{\rm A}$, the smaller value of $H_{\rm A}$ in thinner films is the possible reason for the reduction of $H_{\rm C}$ when t decreases from 10nm. According to the magnetic anisotropy of the LCMO films, the single-domain size and the Bloch domain wall width $\delta_{\rm B}$ of these films are estimated to be about 100nm and 10nm, respectively. These orders of magnitude are consistent with several previous reports.[7,19] Because the grain size is about several hundred nanometres for the films with t >10nm, the low intrinsic coercivity can be due to a multi-domain grain structure besides the low magnetic anisotropy. For films with $t \leq$10nm, a single-domain grain can be expected. As the intrinsic coercivity is less than the magnetic anisotropy, $\alpha_{\rm k}$ in Eq.(2) is less than 1. In other words, there are defect regions in the films. Considering the single-domain structure for thin films, the defect regions are mainly in the grain boundaries. α_k for t =25nm is approximately equal to that for t=10nm according to Eq.(2) using the intrinsic coercivity (shown in Fig.6) and the magnetic anisotropy (shown in Fig.4). However, the coercivity mechanism for t=25nm is differ-

ent from that for t=10nm. As reported in Ref.[20], $r_0/\delta_B \geq 1$ can be concluded for the thin films considering the value of α_k, where r_0 is the width of the magnetic inhomogeneous regions. Therefore, the average width of inhomogeneity regions in the grain boundaries is larger than 10nm.

4. Summary

The effects of strain and film thickness on the coercivity of $La_{0.67}Ca_{0.33}MnO_3$ films grown on $SrTiO_3$ and $LaAlO_3$ substrates have been systematically studied. The magnetic anisotropy is tuned by the strain imposed by the substrate. It is found that the coercivity increases first as t varies from 5nm to 10nm, then attains a maximum value at t ~10–25nm. A further increase of t leads to the gradual reduction of coercivity. By the analysis of the coercivity measured with the magnetic field parallel and perpendicular to the film surface, the coercivity for $t \leq$ 10nm and $t \geq$25nm are mainly controlled by the nucleation of reversed domain and inhomogeneous pinning of domain wall, respectively, which were further confirmed by the initial magnetization curves for the LCMO/STO film with t=5, 10, 25 and 400nm, and the minor magnetic loops of the LCMO/LAO films with t=5 and 50nm. The inhomogeneous region in which nucleation or pinning takes place is mainly localized in the grain boundary and its width is estimated to be greater than 10nm.

References

[1] Jin S, Tiefel T H, McCormack M, Fastnacht R A, Ramesh R and Chen L H 1994 *Science* **264** 413

[2] Jin S, Tiefel T H, McCormack M, O'Bryan H M, Chen L H and Ramesh R 1995 *Appl. Phys. Lett.* **67** 557

[3] Koo T Y, Park S H, Lee K B and Jeong Y H 1997 *Appl. Phys. Lett.* **71** 977

[4] Cai J W, Zhao J G, Zhan W S and Shen B G 1997 *Prog. Phys.* **17** 119 (in Chinese)

[5] Li R W, Wang Z H, Chen X and Shen B G 1999 *Acta Phys. Sin.* **48** S105 (in Chinese)

[6] Lu Y, Li Q A, Di N L, Li R W and Cheng Z H 2003 *Chin. Phys.* **12** 1301

[7] Kwon C, Robson M C, Kim K C, Gu J Y, Lofland S E, Bhagat S M, Trajanovic Z, Rajeswari M, Venkatesan T, Kratz R A, Gomez R D and Ramesh R 1997 *J. Magn. Magn. Mater.* **172** 229

[8] O'Donnell J, Rzchowski M S, Echstein J N and Bozovic I 1998 *Appl. Phys. Lett.* **72** 1775

[9] Steenbeck K, Habisreuther T, Dubourdieu C and Senateur J P 2002 *Appl. Phys. Lett.* **80** 3361

[10] Steren L B, Sirena M and Guimpel J 2000 *J. Appl. Phys.* **87** 6755

[11] Steren L B, Sirena M and Guimpel J 2002 *Phys. Rev.* B **65** 94431

[12] Kronmuller H, Durst K D and Martinek G 1987 *J. Magn. Magn. Mater.* **69** 149

[13] Zhang H W, Sun Z G, Zhang S Y, Han B S, Shen B G, Tung I C and Chin T S 1999 *Phys. Rev.* B **60** 64

[14] Cebollad F, Rossignol M F, Givord D, Villas-Boas V and Gonzalez J M 1995 *Phys. Rev.* B **52** 13511

[15] Suponev N P, Grechishikin R M, Lyakhova M B and Pushkar Yu E 1996 *J. Magn. Magn. Mater.* **157-158** 376

[16] Pawlik P, Wyslocki J J, Kasuwara W and Leonowicz M 2002 *J. Magn. Magn. Mater.* **242-245** 1344

[17] Callegaro L and Puppin E 1995 *Appl. Phys. Lett.* **65** 1279

[18] Zhang H W, Rong C B, Zhang J, Zhang S Y and Shen B G 2002 *Phys. Rev.* B **66** 184436

[19] Lecoeur P, Trouilloud P L, Xiao G, Gupta A, Gong G O and Li W X 1997 *J. Appl. Phys.* **82** 3934

[20] Kronmuller H, Durst K D and Sagawa M 1988 *J. Magn. Magn. Mater.* **74** 291